Theoretical study on quantum effects in triangular antiferromagnets with axial anisotropy using the numerically constructed Bogoliubov transformation for magnons

Y. Watabe
Department of Mathematics and Physical Science, Graduate School of Science and Technology, Chiba University, Yayoi-cho, Inage-ku, Chiba 263, Japan

T. Suzuki and Y. Natsume
Department of Physics, Faculty of Science, Chiba University, Yayoi-cho, Inage-ku, Chiba 263, Japan
(Received 30 December 1994)

Quantum effects expressed by the energy shift ΔE from the Néel energy $E^{\text{Néel}}$ and the spin reduction ΔS for zero-point fluctuations of magnons are investigated theoretically for the triangular antiferromagnets (TLAF) on the xy plane with the one-ion-type axial anisotropy $-|D|(S^z)^2$. We use a method of constructing the canonical transformation without knowledge of the analytical expression called the Bogoliubov transformation. As a result, boson-type excitations are obtained numerically. Here, characteristic properties are discussed in comparison with those for TLAF with the plane-type anisotropy $+|D|(S^z)^2$, for which the canonical transformation can be given in analytical form. Furthermore, the calculation is performed to reveal quantum effects in a six-sublattice structure, which is formed in layered TLAF with the interlayer antiferromagnetic exchange interaction. The behavior of calculated ΔE and ΔS is discussed in the context of magnetic properties of VBr_2, VCl_2, $CsNiBr_3$, and $CsMnI_3$.

I. INTRODUCTION

Though quantum effects in spin systems of antiferromagnetic compounds have not been defined explicitly, expressions of their characteristic features using energy-shift ΔE and spin reduction ΔS due to zero-point quantum fluctuations for magnons have been well confirmed. In fact, the calculations of ΔE and ΔS for two-sublattice Néel states in a square-type lattice, i.e., the collinear spin structure, are the archetype subject in the theory of magnetism in antiferromagnetic compounds.[1]

However, quantum effects in triangular antiferromagnets (TLAF) have not yet been well confirmed because TLAF contain essentially the spin frustration in the three-sublattice structure. In Fig. 1(a), we show the three-sublattice structure A,B,C on the plane. The corresponding first Brillouin zone for this magnetic unit cell is illustrated in Fig. 1(b). It should be noted that the Néel state is a noncollinear structure. In TLAF, therefore, the type of anisotropy plays an essential role in magnetic orderings. Here, we consider the one-ion-type anisotropy. As for TLAF with an anisotropy of the easy-plane type (called TLAF-PL), the 120° Néel structure is well confirmed as shown in Fig. 2(a). The theoretical study of spin-wave expansion from such a 120° Néel structure on the plane has been reported by Oguchi,[2] in connection with the quantum effect ΔS. Furthermore, Jolicoeur and Le Guillou have also discussed[3] ΔE and ΔS in TLAF without any anisotropy, introducing the method of performing a generalized Bogoliubov transformation by the use of symmetric properties of the system. Recently, the effect of interlayer exchange interaction on systems of TLAF-PL has been studied by Welz.[4] In these reports,[2–4] the spiral symmetry of the spin structure enables theoretical investigations using spin waves. Therefore, the analytical canonical transformation (Bogoliubov transformation) can be obtained, which leads us to an easy estimation of quantum effects.

On the other hand, the study of quantum effects in TLAF with an anisotropy of the easy-axis type (called TLAF-AX), whose axis (z axis) is perpendicular to the plane, has not yet been carried out because low-symmetric spin structure [the deformed 120° structure as shown in Fig. 2(b)] prevents the analytical diagonalization of the Hamiltonian, though the magnon dispersion has been thoroughly investigated by Suzuki and Natsume[5] in the context of the explanation for magnetic-resonance properties in VBr_2 (Ref. 6) and VCl_2 (Ref. 7). In the present work, quantum effects in TLAF-AX are investigated on the basis of a method of *numerical* construction for canonical transformation.

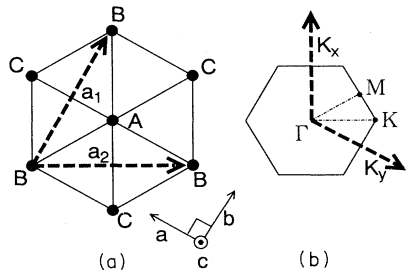

FIG. 1. The three-sublattice structure for the triangular antiferromagnetic system on the c plane. (a) Sublattices A, B, and C are shown on the plane, where arrows $\mathbf{a}_1$ and $\mathbf{a}_2$ are primitive vectors for this unit cell. (b) The corresponding first Brillouin zone for the magnetic unit cell, in which primitive vectors on the reciprocal lattice are indicated by arrows $\mathbf{K}_x$ and $\mathbf{K}_y$.

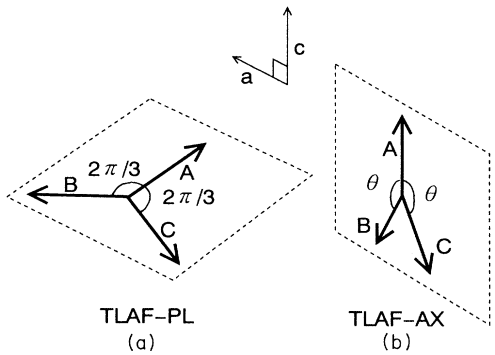

FIG. 2. Néel structure in the three-sublattice structure for the triangular antiferromagnetic system. (a) The 120° structure on the c plane, which is well confirmed in the case where the anisotropy is of the easy-plane type (TLAF-PL). (b) The deformed 120° structure on the ac plane for the case of the easy-axis-type anisotropy (TLAF-AX). The angle θ is larger than $2\pi/3$.

II. MODEL

We discuss the following Hamiltonian for magnetic moments of spins in the present three-sublattice structure;

$$\mathcal{H}=2J\sum_{\langle i,j\rangle}(\mathbf{S}_i\cdot\mathbf{S}_j)-D\sum_i(S_i^z)^2\ , \tag{1}$$

where $\langle i,j\rangle$ takes nearest neighbors (NN's) for $A-B$, $B-C$, and $C-A$ as shown in Fig. 1(a). Situations of $D>0$ and $D<0$ in Eq. (1) correspond to TLAF-AX and TLAF-PL, respectively. The Néel structure is the deformed 120° one on the ac plane for $D>0$ (TLAF-AX) as shown in Fig. 2(b), where angles θ between S_A and S_B (S_C) are determined by

$$\cos\theta=-\frac{1}{2}\left[1-\frac{D}{2Jz}\right]^{-1} \tag{2}$$

for the number z ($=3$) of NN's for sublattices. It is noteworthy that θ is greater than $2\pi/3$ because of the effect of D. As for those for $D<0$ (TLAF-PL), the 120° structure on the c plane [shown in Fig. 2(a)] is well known and has been discussed by several authors.[2–4,8] In fact, in the discussion, the comparison with characteristic features in TLAF-PL is made. In Sec. VI, we extend our study to quantum effects in layered TLAF, where the six-sublattice structure is adopted in consideration of interlayer antiferromagnetic exchange interaction.

III. SPIN-WAVE IN THE EXPRESSION OF HOLSTEIN-PRIMAKOFF TRANSFORMATION

For TLAF-AX, the Holstein-Primakoff formalism transforms the Hamiltonian (1) into

$$\mathcal{H}=E^{\text{Néel}}(1+1/S)+\sum_{\mathbf{k}}X_{\mathbf{k}}^{\dagger}\tilde{\mathcal{H}}_{\mathbf{k}}X_{\mathbf{k}} \tag{3}$$

in the linearized form, where $X_{\mathbf{k}}$ is the following column vector:

$$X_{\mathbf{k}}=[a_{\mathbf{k}},b_{\mathbf{k}},c_{\mathbf{k}},a_{-\mathbf{k}}^{\dagger},b_{-\mathbf{k}}^{\dagger},c_{-\mathbf{k}}^{\dagger}]^t\ . \tag{4}$$

Here, the summation is taken over the magnetic Brillouin zone shown in Fig. 1(b). In $X_{\mathbf{k}}$, a, b, and c are Bose operators for A, B, and C sublattices, respectively. In the Hamiltonian (3), $E^{\text{Néel}}$ is the Néel energy of the following expression:[5]

$$E^{\text{Néel}}=\tfrac{2}{3}zNJS^2(2\cos\theta+\cos2\theta)-\tfrac{1}{3}DNS^2(1+2\cos^2\theta)\ , \tag{5}$$

where N represents the total number of spins. Furthermore, the magnon Hamiltonian matrix $\tilde{\mathcal{H}}_{\mathbf{k}}$ in Eq. (3) is

$$\tilde{\mathcal{H}}_{\mathbf{k}}=2zSJ\frac{1}{2}\begin{bmatrix}\mathcal{E}_{\mathbf{k}} & \mathcal{F}_{\mathbf{k}}\\ \mathcal{F}_{\mathbf{k}} & \mathcal{E}_{\mathbf{k}}\end{bmatrix}\ , \tag{6}$$

in which $\mathcal{E}_{\mathbf{k}}$ and $\mathcal{F}_{\mathbf{k}}$ are the following complex matrices:

$$\mathcal{E}_{\mathbf{k}}=\begin{bmatrix}P & U_+f_{\mathbf{k}}^* & U_+f_{\mathbf{k}}\\ U_+f_{\mathbf{k}} & Q & V_+f_{\mathbf{k}}^*\\ U_+f_{\mathbf{k}}^* & V_+f_{\mathbf{k}} & Q\end{bmatrix}$$

and (7)

$$\mathcal{F}_{\mathbf{k}}=\begin{bmatrix}0 & U_-f_{\mathbf{k}}^* & U_-f_{\mathbf{k}}\\ U_-f_{\mathbf{k}} & W & V_-f_{\mathbf{k}}^*\\ U_-f_{\mathbf{k}}^* & V_-f_{\mathbf{k}} & W\end{bmatrix}\ .$$

In the components of these matrices, $f_{\mathbf{k}}$ is the complex function $(1/z)\Sigma\rho\exp(i\mathbf{k}\cdot\boldsymbol{\rho})$ of wave-vector $\mathbf{k}$ with distance vectors $\boldsymbol{\rho}$ for three NN's. In Eq. (7), functions P, Q, U_-, V_-, U_+, V_+, and W are written as

$$\begin{aligned}P&=-2\cos\theta+2(D/2Jz)\ ,\\ Q&=-(\cos2\theta+\cos\theta)+(D/2Jz)(3\cos^2\theta-1)\ ,\\ U_-&=-(1-\cos\theta)/2\ ,\\ V_-&=-(1-\cos2\theta)/2\ ,\\ U_+&=(1+\cos\theta)/2\ ,\\ V_+&=(1+\cos2\theta)/2\ ,\\ W&=-(D/2Jz)\sin^2\theta\ .\end{aligned} \tag{8}$$

As for TLAF-PL, the Hamiltonian matrix is presented in Ref. 3. In this case, $\mathcal{E}_{\mathbf{k}}$ and $\mathcal{F}_{\mathbf{k}}$ are permutation matrices reflecting the spiral symmetry of spin structure. In contrast, for TLAF-AX, magnons $b_{\mathbf{k}}$ and $c_{\mathbf{k}}$ are no longer equivalent to magnon $a_{\mathbf{k}}$. There remains only the inversion symmetry of $b_{\mathbf{k}}$ and $c_{\mathbf{k}}$.

IV. NUMERICAL APPROACH TO THE CANONICAL TRANSFORMATION: DIAGONALIZATION OF MAGNON HAMILTONIAN

As for TLAF-PL, the canonical transformation for the magnon expression introducing three kinds of boson corresponding to three sublattices has already been obtained analytically by Oguchi[2] as mentioned in Sec. I. Furthermore, Shiba has suggested that it can be also derived using the helical magnon method.[9] This method has also

been recently adopted by Welz.[4]

In general, for TLAF, the transformation $\mathcal{S}_{\mathbf{k}}$ from $X_{\mathbf{k}}$ of Eq. (4) to $Y_{\mathbf{k}}$ for boson basis

$$Y_{\mathbf{k}}=[\alpha_{\mathbf{k}},\beta_{\mathbf{k}},\gamma_{\mathbf{k}},\alpha^{\dagger}_{-\mathbf{k}},\beta^{\dagger}_{-\mathbf{k}},\gamma^{\dagger}_{-\mathbf{k}}]^{t} \tag{9}$$

is written as

$$Y_{\mathbf{k}}=\mathcal{S}_{\mathbf{k}}X_{\mathbf{k}} \ . \tag{10}$$

We should determine the expression of $\mathcal{S}_{\mathbf{k}}$, which diagonalizes $\tilde{\mathcal{H}}_{\mathbf{k}}$, that is

$$(\mathcal{S}^{-1}_{\mathbf{k}})^{\dagger}\tilde{\mathcal{H}}_{\mathbf{k}}\mathcal{S}^{-1}_{\mathbf{k}}=\tfrac{1}{2}\Omega_{\mathbf{k}} \ , \tag{11}$$

under the condition that $\mathcal{S}_{\mathbf{k}}$ is the canonical transformation given by

$$\mathcal{S}_{\mathbf{k}}\mathcal{G}\mathcal{S}^{\dagger}_{\mathbf{k}}=\mathcal{G} \ . \tag{12}$$

Here, the diagonalized matrix $\Omega_{\mathbf{k}}$ is

$$\Omega_{\mathbf{k}}=\begin{bmatrix} \epsilon^{\alpha}_{\mathbf{k}} & & & & & \\ & \epsilon^{\beta}_{\mathbf{k}} & & & 0 & \\ & & \epsilon^{\gamma}_{\mathbf{k}} & & & \\ & & & \epsilon^{\alpha}_{-\mathbf{k}} & & \\ & 0 & & & \epsilon^{\beta}_{-\mathbf{k}} & \\ & & & & & \epsilon^{\gamma}_{-\mathbf{k}} \end{bmatrix} , \tag{13}$$

and $\mathcal{G}$ is the diagonal matrix

$$\mathcal{G}=\begin{bmatrix} \mathcal{I} & \\ & -\mathcal{I} \end{bmatrix} ,$$

where $\mathcal{I}$ is the 3×3 identity matrix. Consequently, we can obtain the magnon-excitation energy as

$$\mathcal{H}=E^{\text{Néel}}+\Delta E+\sum_{\mathbf{k}}[\epsilon^{\alpha}_{\mathbf{k}}\alpha^{\dagger}_{\mathbf{k}}\alpha_{\mathbf{k}}+\epsilon^{\beta}_{\mathbf{k}}\beta^{\dagger}_{\mathbf{k}}\beta_{\mathbf{k}}+\epsilon^{\gamma}_{\mathbf{k}}\gamma^{\dagger}_{\mathbf{k}}\gamma_{\mathbf{k}}] \ . \tag{14}$$

Here, ΔE is the energy shift for zero-point fluctuations of magnons written as

$$\Delta E=\frac{1}{S}E^{\text{Néel}}+\frac{1}{2}\sum_{\mathbf{k}}[\epsilon^{\alpha}_{\mathbf{k}}+\epsilon^{\beta}_{\mathbf{k}}+\epsilon^{\gamma}_{\mathbf{k}}] \ . \tag{15}$$

If we can find the analytical form of $\mathcal{S}_{\mathbf{k}}$ by using the symmetry of the system, we can discuss quantum effects using analytical expressions. In such cases, $\mathcal{S}_{\mathbf{k}}$ is conventionally called Bogoliubov transformation. Indeed, TLAF-PL is a typical example of such cases.

In contrast to this, we have not found the analytical expression of $\mathcal{S}_{\mathbf{k}}$ in the present case of TLAF-AX because of the low symmetry of the spin structure as mentioned at the end of Sec. I. However, we can obtain values of $\epsilon^{\alpha}_{\mathbf{k}}$, $\epsilon^{\beta}_{\mathbf{k}}$, and $\epsilon^{\gamma}_{\mathbf{k}}$ numerically by the method proposed by White, Sparks, and Ortenburger.[10] The equation of motions is

$$i\hbar\dot{X}_{\mathbf{k}}=[X_{\mathbf{k}},\mathcal{H}]=\tilde{\mathcal{L}}_{\mathbf{k}}X_{\mathbf{k}} \ . \tag{16}$$

Here, it should be noted that $\tilde{\mathcal{L}}_{\mathbf{k}}$ written as

$$\tilde{\mathcal{L}}_{\mathbf{k}}=2\mathcal{G}\tilde{\mathcal{H}}_{\mathbf{k}} \tag{17}$$

is not, in general, Hermitian. Inserting (10) into (16), we obtain

$$[Y_{\mathbf{k}},\mathcal{H}]=(\mathcal{S}_{\mathbf{k}}\tilde{\mathcal{L}}_{\mathbf{k}}\mathcal{S}^{-1}_{\mathbf{k}})Y_{\mathbf{k}} \ . \tag{18}$$

Considering that the left-hand side is

$$[Y_{\mathbf{k}},\mathcal{H}]=\mathcal{G}\Omega_{\mathbf{k}}Y_{\mathbf{k}} \ , \tag{19}$$

we can write

$$\mathcal{S}_{\mathbf{k}}\tilde{\mathcal{L}}_{\mathbf{k}}=\mathcal{G}\Omega_{\mathbf{k}}\mathcal{S}_{\mathbf{k}} \ . \tag{20}$$

As a result, we obtain[5] numerical values of $\epsilon^{\alpha}_{\mathbf{k}}$, $\epsilon^{\beta}_{\mathbf{k}}$, and $\epsilon^{\gamma}_{\mathbf{k}}$ as eigenvalues of $\tilde{\mathcal{L}}_{\mathbf{k}}$ without the knowledge of $\mathcal{S}_{\mathbf{k}}$. Consequently, ΔE in Eq. (15) can also be estimated numerically.

Here, it should be noted that the matrix $\mathcal{S}_{\mathbf{k}}$ is not determined uniquely as a result of numerical diagonalization for the non-Hermitian matrix $\tilde{\mathcal{L}}_{\mathbf{k}}$: the coefficient of each row remains indefinite, while magnon excitations have already been uniquely obtained. Thus, we are faced with the problem of how to obtain the canonical transformation. Hereafter, we discuss the method of selecting the exact solutions for the canonical transformation numerically as the central aim of the present work; we construct the canonical transformation using Eq. (12), determining any coefficient under the condition that commutation relations for bosons hold $\alpha_{\mathbf{k}}$, $\beta_{\mathbf{k}}$, and $\gamma_{\mathbf{k}}$, i.e.,

$$[\alpha_{\mathbf{k}},\alpha^{\dagger}_{\mathbf{k}'}]=\delta_{\mathbf{k},\mathbf{k}'},[\beta_{\mathbf{k}},\beta^{\dagger}_{\mathbf{k}'}]=\delta_{\mathbf{k},\mathbf{k}'} \ ,$$

$$[\gamma_{\mathbf{k}},\gamma^{\dagger}_{\mathbf{k}'}]=\delta_{\mathbf{k},\mathbf{k}'},[\alpha_{\mathbf{k}},\beta^{\dagger}_{\mathbf{k}'}]=0 \ ,$$

$$[\beta_{\mathbf{k}},\gamma^{\dagger}_{\mathbf{k}'}]=0 \ ,$$

$$[\gamma_{\mathbf{k}},\alpha^{\dagger}_{\mathbf{k}'}]=0 \ ,$$

etc. As long as we can determine consistent values for these coefficients, we claim that we numerically obtain the exact solutions for the canonical transformation. The mathematical discussion of this method will appear in the general theoretical study in another publication by the present authors.[11] Accordingly, a quantum effect expressed by $\mathcal{S}_{\mathbf{k}}$, for example ΔS, is calculated numerically in cases where the analytical expression for $\mathcal{S}_{\mathbf{k}}$ is unknown.

V. NUMERICAL RESULTS OF MAGNON DISPERSIONS AND QUANTUM EFFECTS

We show the dispersion of magnons in Fig. 3 for both the cases of TLAF-PL and TLAF-AX. These figures have already been reported by several authors.[2,5,8] In particular, the calculation of two-magnon Raman scattering has been performed by the present authors.[8] As for the dispersion in TLAF-PL [Fig. 3(a)],[2,8] the sticking together of three modes at K reflects the symmetry for 120° rotation of spins on the c plane. On the other hand, the sticking together appears at K for only two modes in TLAF-AX [Fig. 3(b)],[5] because of the symmetric property of the exchange between S_B and S_C.

The calculated energy shift ΔE for zero-point quantum fluctuations of magnons is shown in Fig. 4, where the dependence on $D/2J$ is illustrated. It should be noted that ΔE in TLAF-AX has a minimum at $D/2J=0.66\pm0.01$. We remark that the derivative at

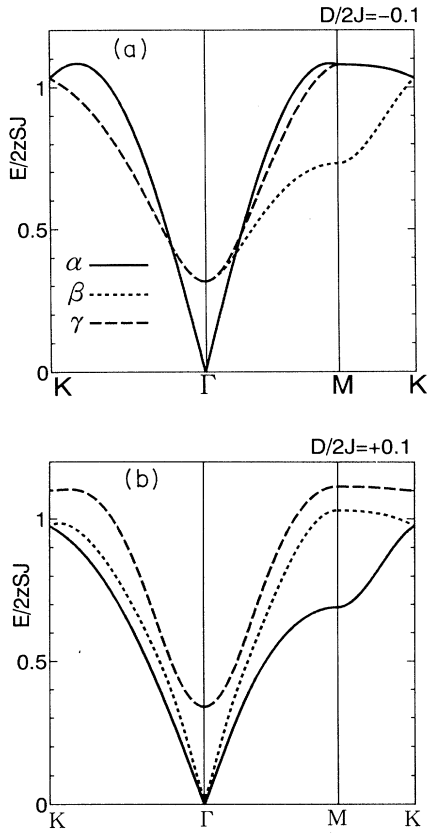

FIG. 3. Calculated dispersions of magnons for $|D|/2J=0.1$. (a) The dispersion in the first Brillouin zone illustrated in Fig. 1(b) for TLAF-PL ($D/2J=-0.1$). Discussions on properties of modes α, β, and γ have appeared in previous papers (Refs. 2 and 8). (b) The dispersion for TLAF-AX ($D/2J=+0.1$). The character of each mode has been reported in our previous study (Ref. 5).

$D/2J=1.5$ is not continuous for TLAF-AX because the spin state changes from the noncollinear structure to the collinear one. Furthermore, the dependence of $E^{\text{Néel}}$ and $E_g=E^{\text{Néel}}+\Delta E$ on $D/2J$ is also shown in Fig. 4. The discontinuity of the derivative at $D/2J=1.5$ is also seen in the behavior of E_g.

In comparison with ΔE, the zero-point spin reduction ΔS is seriously affected by characteristics of magnon dispersion around $\mathbf{k}=0$. In fact, Fig. 5 shows the dependence of ΔS_A $(=\Delta S_B=\Delta S_C)$ in TLAF-PL and $\Delta S_A, \Delta S_B$ $(=\Delta S_C)$ in TLAF-AX on $D/2J$. The value for any ΔS becomes 0.26 at $D/2J=0$, which agrees with the result in Refs. 2 and 3. The discontinuity of derivatives at $D/2J=1.5$ is also seen in ΔS_B and ΔS_C corresponding to that of ΔE. It should be pointed out that the value of spin reduction is essentially dependent on sublattices, as expected from the spin configuration without the spiral symmetry. In detail, ΔS_B $(=\Delta S_C)$ is significantly larger than ΔS_A in the region of $0<D/2J\lesssim 1$, because fluctuations of S_B $(=S_C)$ are promoted more than those of S_A due to the competition between J and D. In contrast, ΔS_B $(=\Delta S_C)$ becomes smaller than ΔS_A for $D/2J\geq 1.3\pm 0.05$, reflecting the precursor of collinear structure for $D/2J\geq 1.5$. In the collinear structure, we would like to point out that the spin reduction makes no contribution to the total magnetization, i.e., $\Delta S_A=\Delta S_B+\Delta S_C$. The characteristic behavior of ΔE and ΔS_i in TLAF-AX discussed here can be obtained by introducing the method proposed in the preceding section.

VI. SIX-SUBLATTICE STRUCTURE

In this section, we adopt the present method to the investigation of quantum effects ΔE and ΔS_i in the six-sublattice structure, which is formed in layered TLAF with the interlayer antiferromagnetic exchange interac-

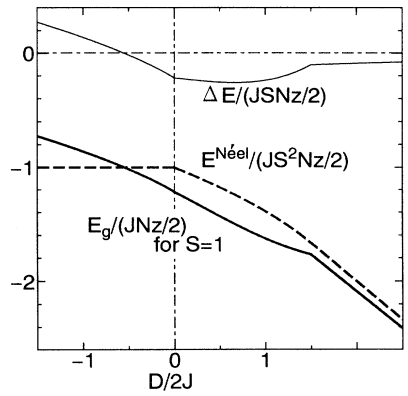

FIG. 4. Calculated energy shift ΔE for zero-point quantum fluctuations of magnons shown by the thin line. The unit is $JSNz/2$. Furthermore, Néel energy $E^{\text{Néel}}$ is shown by the dashed line, the unit of which is $JS^2Nz/2$. The sum of these two values is shown by the thick line of $E_g/(JNz/2)$, where we use $S=1$.

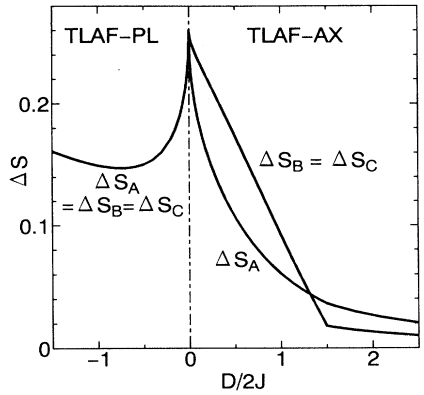

FIG. 5. The zero-point spin reduction ΔS_i shown for each sublattice for both cases of TLAF-PL ($D/2J<0$) and TLAF-AX ($D/2J>0$). For TLAF-PL, ΔS_i has the common value of S_A, S_B, and S_C. Such behavior has been reported by several authors (Refs. 2 and 3). For TLAF-AX, ΔS_A has a different value from ΔS_B $(=\Delta S_C)$. The behavior of each ΔS_i for TLAF-AX is reported for the first time.

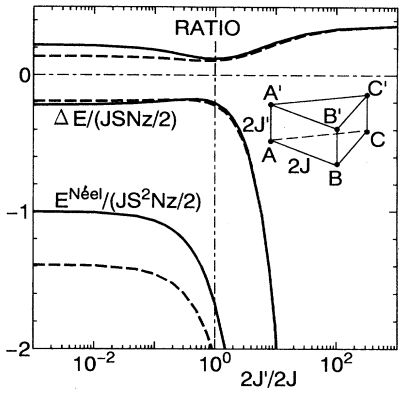

FIG. 6. The dependence of $\Delta E/(JSNz/2)$ and $E^{\text{Néel}}/(JS^2Nz/2)$ for a six-sublattice structure on $2J'/2J$ are shown by solid line for $D/2J=0$ and by dashed line for $D/2J=1.0$. Furthermore, the ratios of $\Delta E/(JSNz/2)$ to $E^{\text{Néel}}/(JS^2Nz/2)$ obtained using $S=1$ are illustrated by solid (dashed) lines for $D/2J=0$ (1.0) in the upper part of the figure. The value of 10^0 for $2J'/2J$ corresponds to the three-dimensional system. The six-sublattice structure for the layered TLAF is schematically illustrated in the inset.

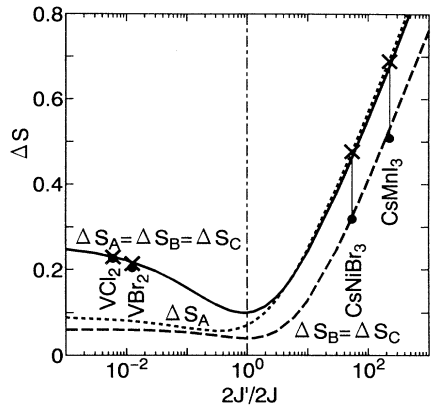

FIG. 7. The zero-point spin reductions $\Delta S_A=\Delta S_B=\Delta S_C$ for six-sublattice structure vs $2J'/2J$ are shown by the solid line for $D/2J=0$. Furthermore, ΔS_A and $\Delta S_B=\Delta S_C$ for $D/2J=1.0$ are shown by the dotted line and the dashed line, respectively. Furthermore, crosses indicate expected values of ΔS_A for VBr_2, VCl_2, $CsNiBr_3$, and $CsMnI_3$, while closed circles indicate those of ΔS_B $(=\Delta S_C)$ for the same compounds. Values of $D/2J$ for those compounds are described in the text, which are determined from experimental reports (Refs. 6, 7, 12, and 13).

tion $2J'$. The Hamiltonian discussed in this section is described as

$$\mathcal{H}=2J\sum_{\langle i,j\rangle}(\mathbf{S}_i\cdot\mathbf{S}_j)+2J'\sum_{\langle i,j\rangle}{}'(\mathbf{S}_i\cdot\mathbf{S}_j)-D\sum_i(S_i^z)^2 \qquad (21)$$

for spins S_A, S_B, S_C on a layer and $S_{A'}$, $S_{B'}$, $S_{C'}$ on the adjacent layer. The schematic illustration of the six-sublattice structure is given in the inset of Fig. 6. Here, $\sum'$ means the summation for interlayer NN's, i.e., $A-A'$, $B-B'$, and $C-C'$. The calculation for this six-sublattice structure is the natural extension of the discussion in Secs. II, III, and IV; directions of spins $S_{A'}$, $S_{B'}$, and $S_{C'}$ are opposite to those of S_A, S_B, and S_C, respectively.

As a result of the numerical calculation, Fig. 6 illustrates the dependence of ΔE and $E^{\text{Néel}}$ on $2J'/2J$, where $D/2J$ is fixed to be 0 or 1.0. Near $2J'/2J=1.0$, where the system becomes the perfect three-dimensional antiferromagnet, ΔE has a maximum. In the region of the one-dimensional antiferromagnet, i.e., $2J'/2J\gg1$, ΔE decreases quite rapidly with increasing $2J'/2J$. This is the characteristic quantum effect for a one-dimensional system.

In addition, we show characteristic features of ΔS_i in Fig. 7. It is easily seen that $\Delta S_{A'}=\Delta S_A$, $\Delta S_{B'}=\Delta S_B$, and $\Delta S_{C'}=\Delta S_C$. In this figure, ΔS_A $(=\Delta S_B=\Delta S_C)$ is shown for $D/2J=0$ by the solid line. This line indicates ΔS both for layered TLAF-PL and layered TLAF-AX. As for the case of $D/2J=1.0$, ΔS_A and $\Delta S_B=\Delta S_C$ are also illustrated by dotted and dashed lines, respectively, i.e., values of spin reduction for layered TLAF-AX are calculated. Values for ΔS_i in the two-dimensional region for $2J'/2J\ll1$ show marked decrease with increasing $2J'/2J$. However, this becomes logarithmic increase, as $2J'/2J$ increases in the one-dimensional region $2J'/2J\gg1$. As a result, this rapid enhancement of ΔS_i for $2J'/2J\gg1$ reflects the well-confirmed[1] quantum effect in one-dimensional magnets.

The corresponding values for ΔS_i in magnetic compounds are also indicated in Fig. 7; two-dimensional triangular lattices VBr_2 (Ref. 6) [VCl_2 (Ref. 7)] have values of $2J'/2J=0.0125$ (0.006) and $D/2J=0.014$ (0.002 27) for spin$=\frac{3}{2}$. On the other hand, the one-dimensional antiferromagnet $CsNiBr_3$ (Ref. 12) has $2J'/2J=54.8$ and $D/2J=1.05$ for spin$=1$. Furthermore, $2J'/2J=226.19$ and $D/2J=1.19$ are reported for $CsMnI_3$ (Ref. 13) for spin$=\frac{5}{2}$.

In order to understand quantum effects in connection with the dimensionality of compounds on the basis of the unified picture obtained systematically by the proposed method, measurements of ΔS_i by neutron scattering[14] are desirable.

Quite recently, experimental study of magnetic phase transition in mixed compounds $Rb_{1-x}K_xNiCl_3$ has been reported by Tanaka, Hasegawa, and Nagata.[15] In this remarkable system, a mixture of $S=1$ Heisenberg antiferromagnets on a deformed triangular lattice (DTLAF) is realized with the easy-axis and easy-plane types of anisotropy. Values of $2J'/2J$ are reported to be 125.26 [in detail, $2J'=23.8$ K, $2J=0.38$ K, and $D=0.024$ (Ref. 16)] for $x=0$ and 1071.4 [$2J'=15.0$ K, $2J=0.028$ K, and $D=-0.86$ (Ref. 17)] for $x=1$. Measurements have been made of susceptibilities and torques for $0\le x\le0.78$. In the context of our theoretical work, it should be noted that the phase transition from DTLAF-AX to DTLAF-PL appears at $x=0.38$ with increasing x. On the basis of our results, the splitting of spin reductions among sublattices is expected at around $x=0.38$. We look forward to measurements of ΔS_i by neutron-scattering experiments in this system.

ACKNOWLEDGMENT

We would like to thank Dr. T. Nakayama of Chiba University for valuable discussions.

[1]For example, D. C. Mattis, *The Theory of Magnetism I* (Springer-Verlag, Berlin, 1981); T. Oguchi, *The Statistical Theory of Magnetic Materials* (Shoukabou, Tokyo, 1970).

[2]T. Oguchi, J. Phys. Soc. Jpn. Suppl. **52**, 183 (1983).

[3]T. Jolicoeur and J. C. Le Guillou, Phys. Rev. B **40**, 2727 (1989).

[4]D. Welz, J. Phys. Condens. Matter **5**, 3643 (1993).

[5]T. Suzuki and Y. Natsume, J. Phys. Soc. Jpn. **56**, 1577 (1987). In this work, the effect of the dynamical coupling with nuclear spins on spin resonance spectra is discussed in VBr_2 and VCl_2.

[6]H. Kadowaki, K. Ubukoshi, and K. Hirakawa, J. Phys. Soc. Jpn. **54**, 363 (1985).

[7]H. Kadowaki, K. Ubukoshi, K. Hirakawa, J. L. Martínez, and G. Shirane, J. Phys. Soc. Jpn. **56**, 4027 (1987).

[8]Y. Watabe, T. Suzuki, and Y. Natsume, J. Phys. Condens. Matter **6**, 7763 (1994). In this work, characteristic features in magnon Raman spectra are discussed for the TLAF-PL.

[9]H. Shiba (private communication). The single boson is introduced to express magnon excitations.

[10]R. M. White, M. Sparks, and I. Ortenburger, Phys. Rev. **139**, A450 (1965).

[11]Y. Watabe, T. Suzuki, and Y. Natsume (unpublished).

[12]S. Maegawa, T. Kohmoto, T. Goto, and N. Fujiwara, Phys. Rev. B **44**, 12 617 (1991).

[13]T. Inami, K. Kakurai, H. Tanaka, M. Enderle, and M. Steiner, J. Phys. Soc. Jpn. **63**, 1530 (1994).

[14]G. E. Bacon, *Neutron Diffraction,* 3rd ed. (Clarendon, Oxford, 1975).

[15]H. Tanaka, T. Hasegawa, and K. Nagata, J. Phys. Soc. Jpn. **62**, 4053 (1993).

[16]K. Nakajima, K. Kakurai, H. Hiraka, H. Tanaka, K. Iio, and Y. Endoh, J. Phys. Soc. Jpn. **61**, 3355 (1992).

[17]H. Tanaka, Y. Kaahwa, T. Hasegawa, M. Igarashi, S. Teraoka, K. Iio, and K. Nagata, J. Phys. Soc. Jpn. **58**, 2930 (1989).